Progress In Electromagnetics Research Letters, Vol. 111, 103–110, 2023

A Compact Tunable Microstrip Bandpass Filter with Tuning Range and Bandwidth Enhancement

Shuang Li*, Shengxian Li, Jun Liu, and Neng Zhang

Abstract—This letter presents a compact constant absolute bandwidth (ABW) frequency tunable bandpass filter (BPF) with bandwidth and tuning range enhancement. The fundamental structure consists of two varactor-loaded step-impedance resonators (SIRs) and input/output feeding lines. By adjusting the position of varactors, the slope of coupling coefficient between the two resonators can be changed easily, which is crucial to realizing constant ABW. The tuning range is improved due to the application of varactor-loaded SIR. To expand the bandwidth, interdigital coupling structures between varactor-loaded SIRs are adopted. Besides, source-load coupling is introduced, and two transmission zeroes (TZs) are generated on both sides of the passband to enhance the rejection level of stopband. The measured results show that the proposed BPF achieves a center frequency tuning range from 0.79 to 1.2 GHz (41.2%), and the 3-dB ABW remains 108 ± 5 MHz. The insertion loss (IL) is 1.8–2.2 dB, and the return loss is greater than 10 dB during the whole tuning range.

1. INTRODUCTION

With the development of wireless communication technology, modern wireless communication systems have a greater number of communication protocols and frequency bands than before. Consequently, communication devices must support multi-bands. In order to realize multi-bands compatibility, numerous fixed frequency filters are utilized with the disadvantages of large size and high cost. As a potential alternative, electronically tunable microwave bandpass filters based on varactor diodes have been appealing due to its advantages of compact size, low cost, low complexity, and fast tuning speed [1].

In recent years, a large number of frequency tunable BPFs have been designed to realize high-flexibility RF front end [2–10]. In [2–5], frequency tunable bandpass filters are obtained based on quarter-wavelength resonators or T-shaped resonators, whereas the absolute bandwidth of filters cannot keep stable over the tuning range, which is important in some practical applications. In [6–8], the tunable BPFs with constant ABW and high selectivity are designed by adopting frequency-dependent coupling structures; however, the filters can only work for narrow-band systems because of their poor bandwidth performance. In [9], a two-pole tunable BPF with constant ABW and reconfigurable TZs is presented, but tuning range of the presented filter is not wide. In [10], a tunable BPF is proposed with a relative bandwidth of 15% by adopting defected ground structures; nevertheless, the selectivity performance of the proposed tunable filter is poor. Consequently, the design of a constant ABW frequency tunable filter with bandwidth and tuning range enhancement is still a challenge.

In this letter, a compact constant ABW tunable bandpass filter with bandwidth and tuning range enhancement is proposed. The proposed tunable filter consists of two varactor-loaded SIRs. Different from the conventional varactor loaded SIR, the varactor in this letter is loaded in the high impedance line of SIR. Due to this design, the slope of the coupling coefficient between the resonators can be changed easily by adjusting the loading position of the varactor, which is very useful for achieving constant ABW.

Received 19 June 2023, Accepted 14 July 2023, Scheduled 26 July 2023
* Corresponding author: Shuang Li (lishuang8118@163.com).
The authors are with the China Academy of Space and Technology (Xi'an), China.

Besides, the tuning range of the filter is improved as a result of the application of varactor loaded SIR. Moreover, the interdigital coupling structures between the two resonators are utilized to expand the bandwidth of the tunable filter. To improve the rejection level of stopband, source-load coupling is introduced, and two TZs are generated at the lower and upper stopband. The layout of the proposed tunable filter is depicted in Fig. 1.

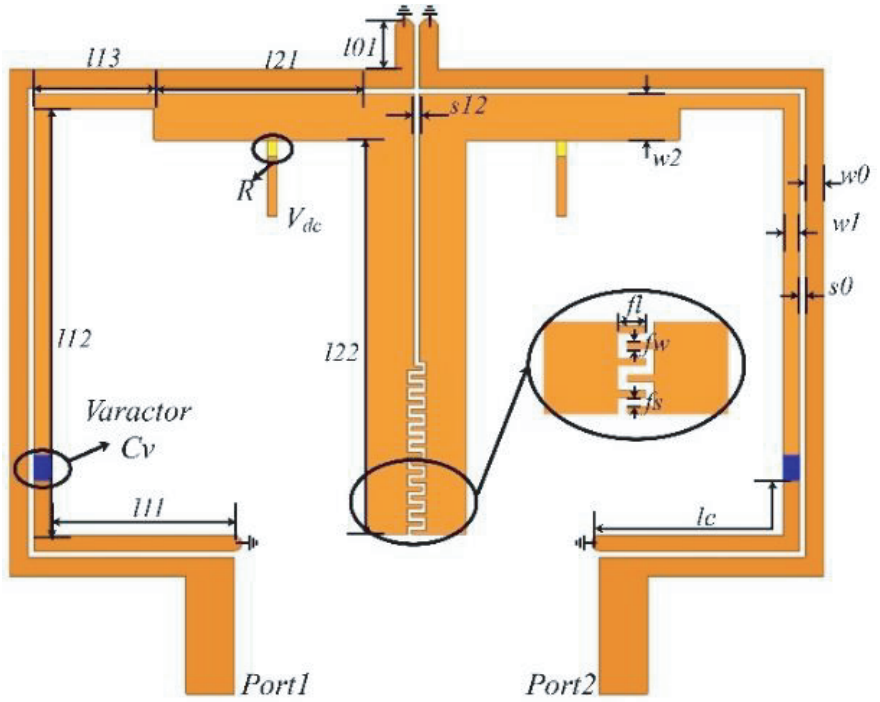

Figure 1. Layout of the proposed tunable filter.

2. ANALYSIS OF VARACTOR-LOADED SIR

The layout of the varactor-loaded SIR is shown in Fig. 2(a). The proposed tunable SIR consists of a high-admittance transmission line, a low-admittance transmission line, and a varactor diode. The characteristic admittance and electrical length of the high/low-admittance transmission line are Y_1, Y_2 and $\theta 1$, $\theta 2$. The varactor diode is loaded at the low-admittance transmission line, and θc is the electrical length between the location of varactor and the short-end of the low-admittance transmission line. Cv is the effective capacitance of varactor diode.

According to the transmission line theory [11], the input admittance Y_{in} of the tunable SIR can be calculated by the following equations, where ω is the angular frequency.

$$Y_A = \frac{Y_2}{j \tan \theta_c} \tag{1}$$

$$Y_B = \frac{jY_1Y_2 \tan\theta_1 + jY_2^2 \tan(\theta_2 - \theta_c)}{Y_2 - jY_1 \tan\theta_1 \tan(\theta_2 - \theta_c)} \tag{2}$$

$$Y_{in} = \frac{jwC_vY_A}{Y_A + jwC_v} + Y_B \tag{3}$$

From the resonance condition, the imaginary part of the input admittance Y_{in} should be zero, and the resonance frequency of the tunable SIR can be calculated by Equations (1)–(3).

For frequency tunable BPFs, tuning range (TR) is an important characteristic, which is defined as Equation (4), where $f(Cv\_\min)$ and $f(Cv\_\max)$ represent resonance frequency when efficient

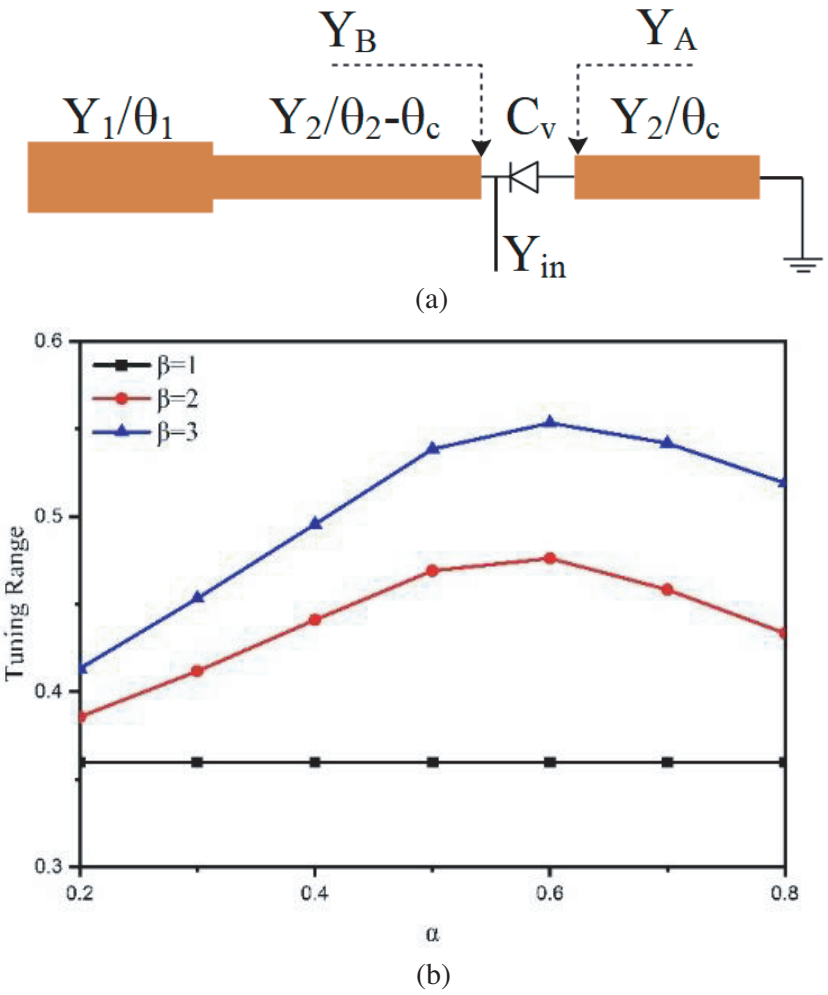

Figure 2. (a) Layout of the varactor-loaded SIR; (b) Tuning range of the tunable SIR versus α with different characteristic impedance β, $Y_1 = 0.03\,\mathrm{S}$, $\theta 1 + \theta 2 = 180^\circ$ where the reference frequency is 1 GHz.

capacitance Cv is minimum and maximum, respectively.

$$TR = \frac{f(C_{v\_\min}) - f(C_{v\_\max})}{(f(C_{v\_\min}) + f(C_{v\_\max}))/2} \tag{4}$$

From Equations (1)–(3), the characteristic admittance and electrical length of the transmission line also affect the resonance frequency of the tunable resonator. Accordingly, the electrical length ratio α and characteristic admittance ratio β can be defined as follows.

$$\alpha = \frac{\theta_2}{\theta_1 + \theta_2} \tag{5}$$

$$\beta = \frac{Y_1}{Y_2} \tag{6}$$

Figure 2(b) shows the relationships between TR and electrical length ratio α under different characteristic admittance ratios β. If the characteristic admittance ratio of the tunable SIR is chosen as $\beta = 1$, the resonator will be transformed into a uniform-impedance resonator (UIR), and TR remains constant as electrical length ratio α changes. To acquire characteristic of the tunable SIR, the scenarios of $\beta = 2$ and $\beta = 3$ are also discussed. The TR increases when the characteristic admittance ratio β increases, which means that the tunable SIR has wider TR than conventional UIR. When electrical

length ratio α increases, TR changes significantly, and the maximum value of TR occurs at around $\alpha = 0.6$.

As can be concluded from above discussions, the proposed tunable SIR can obtain a wider tuning range than conventional UIR. Besides, the slope of coupling coefficient between the proposed varactor-loaded SIRs can be changed easily by adjusting the locating position of varactors, and this feature will be demonstrated in Section 3. Consequently, the tunable SIR is used to design the constant ABW tunable BPF.

3. DESIGN OF COMPACT TUNABLE BPF

In this section, a compact constant ABW tunable BPF based on varactor-loaded SIR is designed and fabricated to verify the above discussion. The dielectric substrate used in the design is a 0.787 mm thick Rogers RT/duroid 5880 substrate with a dielectric constant of 2.2 and a loss tangent of 0.002. The commercial varactor SMV1413 from Skyworks is chosen as the tuning elements with a tuning range from 1.77 to 9.6 pf. The resistor R connected the bias lines and SIRs is 100 k ohm.

To broaden the bandwidth of the tunable bandpass filter, the interdigital coupling structure between the two varactor-loaded SIRs is utilized. Compared with a traditional parallel slot coupling structure, the interdigital coupling structure can significantly improve the coupling capacitance between the two resonators, hence achieving stronger capacitive coupling. Fig. 3 depicts the comparison of coupling coefficient k12 between interdigital coupling structure and traditional parallel slot coupling structure with the same slot size. It can be seen that the interdigital coupling structure can achieve greater coupling coefficient with the same slot size. Based on the classical filter theory, larger coupling coefficient can realize wider bandwidth performance.

As an experimental prototype, a tunable BPF is designed with ABW of 100 MHz; the tuning range of the proposed filter is 0.8–1.2 GHz; two transmission zeros operating at ± 5 (normalized frequency)

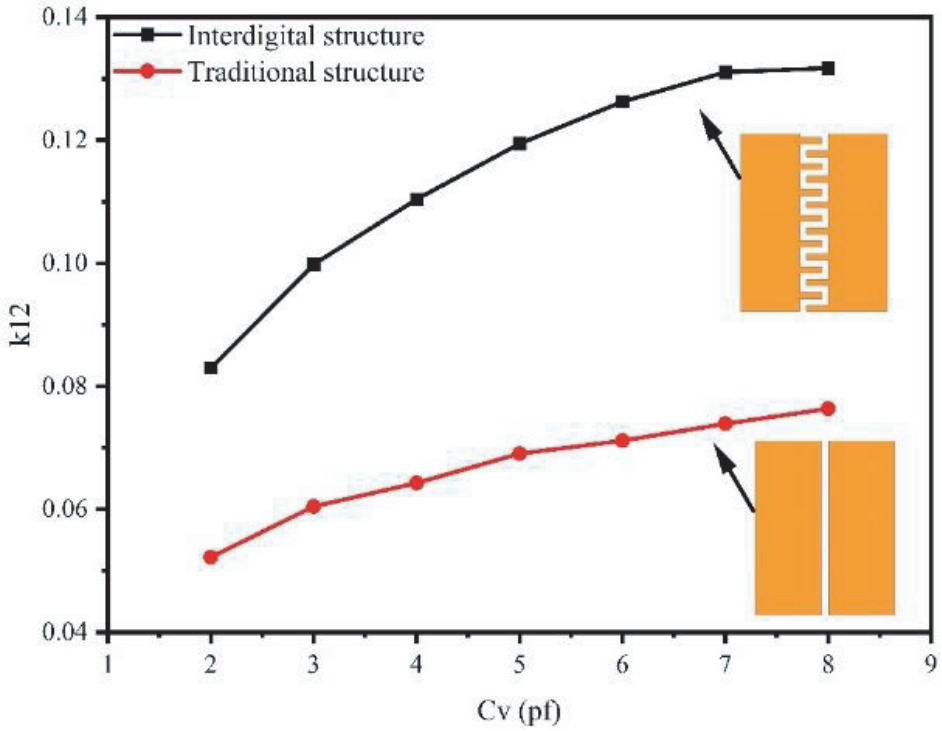

Figure 3. Coupling coefficient k12 versus efficient capacitance Cv with the proposed interdigital coupling structure and traditional coupling structure.

are designed. The normalized coupling matrix $[M]$ of the proposed filter can be synthesized as [11].

$$[M]=\begin{bmatrix} 0 & 1.158 & 0 & -0.1 \\ 1.158 & 0 & 1.667 & 0 \\ 0 & 1.667 & 0 & 1.158 \\ -0.1 & 0 & 1.158 & 0 \end{bmatrix} \tag{7}$$

Then, the desired coupling coefficient k_{12} between resonators and external quality Q_{eS}, Q_{eL} can be obtained by Equations (8)–(9).

$$k_{12} = M_{12} \cdot \frac{ABW}{f_0} \tag{8}$$

$$\begin{aligned} Q_{eS} &= \frac{f_0}{M_{S_1}^2 \cdot ABW} \\ Q_{eL} &= \frac{f_0}{M_{2L}^2 \cdot ABW} \end{aligned} \tag{9}$$

The position of varactor diode, denoted by lc, is a crucial parameter for achieving constant ABW feature of the tunable BPF. Fig. 4 depicts the coupling coefficient k12 and Qe curve versus effective capacitance Cv of varactor diode with different locations lc. As can be seen, the position of varactor can effectively change the variation slope of k12 and Qe against different Cv values. By properly adjusting the position lc, the values of k12 and Qe can satisfy the requirement of constant ABW.

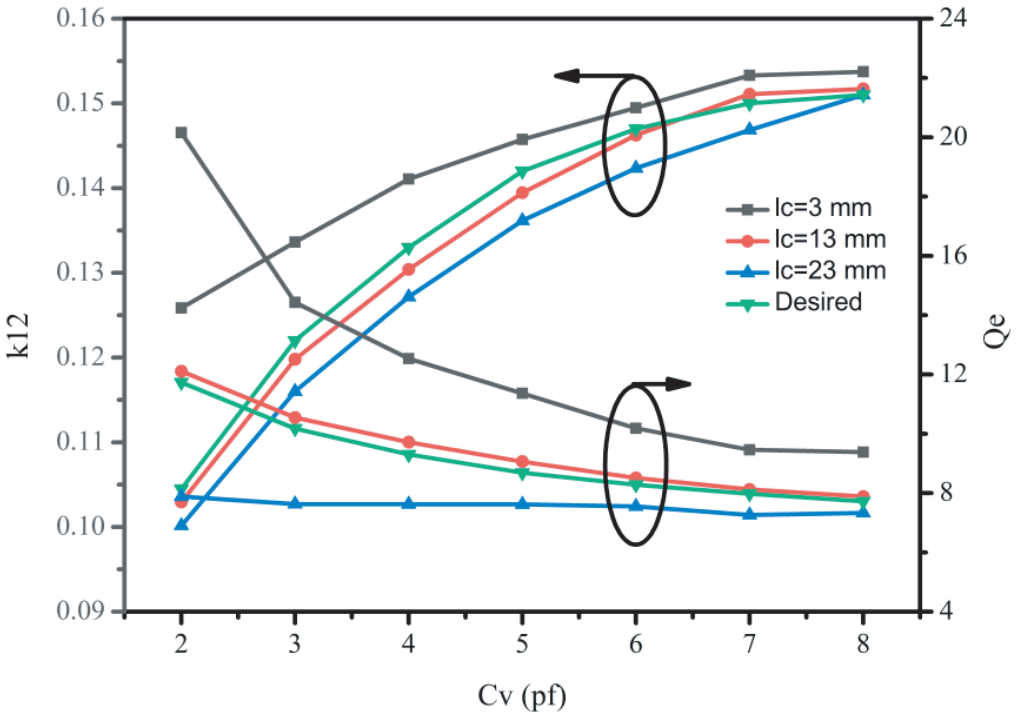

Figure 4. Coupling coefficient k12 and External quality Qe versus efficient capacitance Cv with different locating position lc.

The constant ABW tunable BPF with bandwidth and tuning range enhancement is optimized using full-wave EM simulator HFSS (High Frequency Structure Simulator). Final dimensions are as follows: $w0 = 0.93\,\text{mm}$, $w1 = 0.77\,\text{mm}$, $w2 = 2.31\,\text{mm}$, $s0 = 0.1\,\text{mm}$, $s12 = 0.13\,\text{mm}$, $l11 = 9.2\,\text{mm}$, $l12 = 21.3\,\text{mm}$, $l21 = 10.7\,\text{mm}$, $l22 = 19.7\,\text{mm}$, $fl = 0.9\,\text{mm}$, $fw = 0.2\,\text{mm}$, $fs = 0.2\,\text{mm}$, $lc = 12.8\,\text{mm}$. The overall filter dimension is $40.2\,\text{mm} \times 26.9\,\text{mm}$ ($0.14\lambda g \times 0.1\lambda g$, where λg is the guided wavelength at $f = 0.79\,\text{GHz}$). A photograph of the fabricated tunable BPF is shown in Fig. 5(a).

Figure 5(b) shows the simulated and measured frequency responses of the proposed filter with different bias voltages V_{dc}. As can be seen, the center frequency of the proposed filter can be adjusted

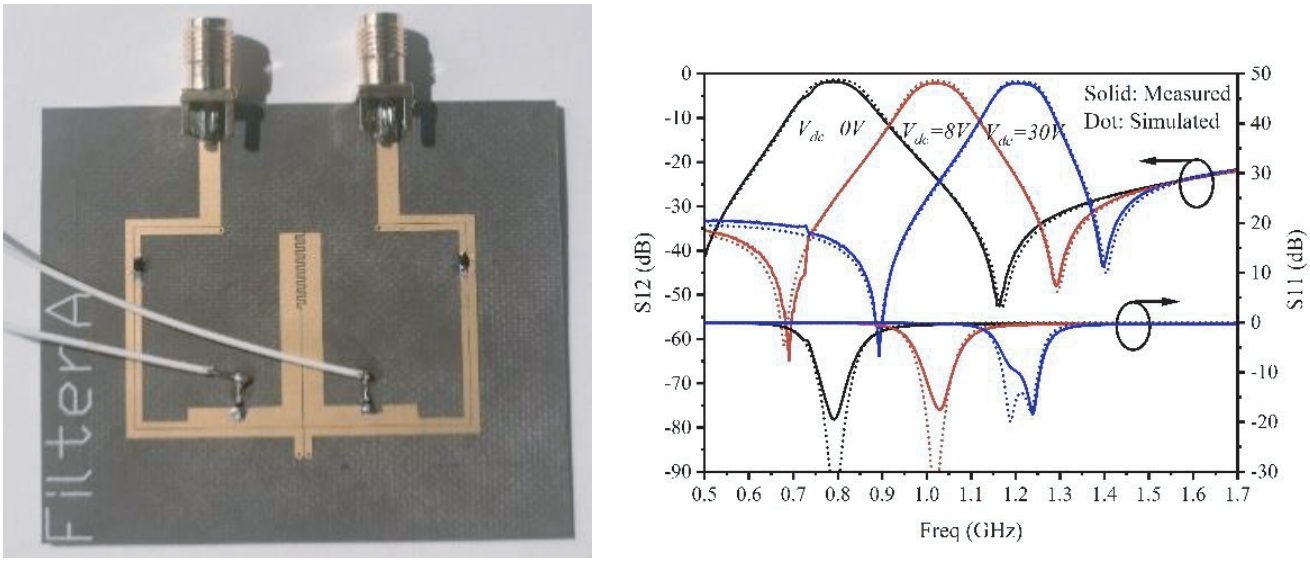

(a) (b)

Figure 5. (a) Photograph of the proposed tunable BPF; (b) Simulated and measured frequency response of the proposed tunable BPF.

from 0.79 to 1.2 GHz with bias voltage V_{dc} changing from 0 to 30 V, and the tuning rate is 41.2%. During the whole tuning range, the 3 dB ABW of the filter remains 108 ± 5 MHz; the insertion loss (IL) is 1.8–2.2 dB; and return loss is greater than 10 dB. Due to the cross-coupling between the input and output (I/O) feeding transmission lines, two self-adaptive TZs are generated on both sides of the passband, and the selectivity of the proposed filter is enhanced significantly. In summary, the simulated and measured results with good agreement show excellent performance in terms of bandwidth and selectivity.

The proposed compact constant ABW tunable BPF is compared with previous tunable BPFs as summarized in Table 1. As can be seen, the proposed tunable filter is competitive in terms of absolute bandwidth, tuning range, number of TZs, and layout size.

Table 1. Key performance comparisons with related works.

REF.	Freq. (GHz)	TR (%)	BW (MHz)	IL (dB)	Order/TZ	Varactors	Size ($\lambda g \times \lambda g$)
[5]	0.8–1.02	24.2	NG	1.1–2.9	4/3	4	NG
[6]	2.3–3.4	38	54*	1.5–2.8	2/2	2	0.25×0.15
[7]	0.89–1.13	23.8	46.8*	3.2–4.3	4/2	4	0.23×0.19
[8]	0.57–0.79	32	51*	2.5–4.1	2/2	4	0.1×0.08
[12]	0.7–1.03	38	65#	1.7–1.8	4/0	4	0.15×0.1
[13]	1.16–1.49	24.9	70*	2	2/0	2	NG
[14]	1.24–1.72	32.4	94.5*	4.6–5.4	4/4	4	NG
[15]	0.8–1.14	35.1	47*	2.7–3.1	4/4	4	0.14×0.17
[16]	1.48–1.88	23	92*	4.8–5.6	5/2	5	NG
T.W.	0.79–1.2	41.2	108*	1.8–2.2	2/2	2	0.14×0.1

Note: T.W.: This Work; *: 3 dB bandwidth, #: 1 dB bandwidth; NG: Not Given.

4. CONCLUSION

A compact constant ABW frequency tunable BPF based on varactor-loaded SIR is proposed in this letter. The desired coupling coefficient slope to achieve constant ABW can be obtained easily by adjusting the position of the varactor. Besides, the tuning range of the filter is improved by adopting varactor loaded SIR. The interdigital coupling structures can expand bandwidth of the filter efficiently. Two TZs at both sides of the passband can be generated by introducing cross-coupling between the input and output feeding lines, which can enhance rejection level of stopband. The simulated and measured results are shown with good agreement. The excellent bandwidth and tuning range performance of the proposed filter make it attractive in modern wireless communication system.

REFERENCES

1. Islam, H., S. Das, T. Bose, and T. Ali, "Diode based reconfigurable microwave filters for cognitive radio applications: A review," *IEEE Access*, Vol. 8, 185429–185444, 2020.
2. Gao, L., T.-W. Lin, and G. M. Rebeiz, "Design of tunable multi-pole multi-zero bandpass filters and diplexer with high selectivity and isolation," *IEEE Transactions on Circuits and Systems I: Regular Papers*, Vol. 66, No. 10, 3831–3842, Oct. 2019.
3. Gao, L. and G. M. Rebeiz, "A 0.97–1.53-GHz tunable four-pole bandpass filter with four transmission zeroes," *IEEE Microwave and Wireless Components Letters*, Vol. 29, No. 3, 195–197, Mar. 2019.
4. Chen, Z. H. and Q. X. Chu, Wideband fully tunable bandpass filter based on flexibly multi-mode tuning," *IEEE Microwave & Wireless Components Letters*, Vol. 26, No. 10, 789–791, 2016.
5. You, B., L. Chen, Y. Liang, and X. Wen, "A high-selectivity tunable dual-band bandpass filter using stub-loaded stepped-impedance resonators," *IEEE Microwave & Wireless Components Letters*, Vol. 24, No. 11, 736–738, 2014.
6. Abdelfattah, M., R. Zhang, and D. Peroulis, "High-selectivity tunable filters with dual-mode SIW resonators in an L-shaped coupling scheme," *IEEE Transactions on Microwave Theory and Techniques*, Vol. 67, No. 12, 5016–5028, Dec. 2019.
7. Ohira, M., S. Hashimoto, Z. Ma, and X. Wang, "Coupling-matrix-based systematic design of single-DC-bias-controlled microstrip higher order tunable bandpass filters with constant absolute bandwidth and transmission zeros," *IEEE Transactions on Microwave Theory and Techniques*, Vol. 67, No. 1, 118-128, Jan. 2019.
8. Zhang, Y.-J., J. Cai, and J.-X. Chen, "Design of novel reconfigurable filter with simultaneously tunable and switchable passband," *IEEE Access*, Vol. 7, 59708–59715, 2019.
9. Kumar, N., S. Narayana, and Y. K. Singh, "Constant absolute bandwidth tunable symmetric and asymmetric bandpass responses based on reconfigurable transmission zeros and bandwidth," *IEEE Transactions on Circuits and Systems II: Express Briefs*, Vol. 69, No. 3, 1014–1018, Mar. 2022.
10. Wünsche, R., R. Collmann, M. Krondorf, and J. Forster, "Microstrip combline bandpass filter with tuning range enhancement and bandwidth tunability using resonator loaded series varactor and SLR," *2022 14th German Microwave Conference (GeMiC)*, 148–151, Ulm, Germany, 2022.
11. Hong, J.-S. and M. J. Lancaster, *Microstrip Filter for RF/Microwave Application*, Wiley, New York, NY, USA, 2001.
12. Liu, Y., L. Liu, C. Liang, and I. Majid, "Compact planar tunable filter with constant absolute bandwidth and wide-frequency tuning range using DGS coupling structure," *IEEE Access*, Vol. 9, 157259–157266, 2021.
13. Dyussembayev, A. and D. Psychogiou, "Continuously tunable 3-D printed helical resonators and bandpass filters using actuated liquid metals," *IEEE Microwave and Wireless Components Letters*, Vol. 32, No. 7, 855–858, Jul. 2022.
14. Lu, D., X. Tang, M. Li, and N. S. Barker, "Four-pole frequency agile bandpass filter with fully canonical response and constant ABW," *IEEE MTT-S Int. Microw. Symp. Dig.*, 1–3, Chengdu, China, May 2018.

15. Li, S., S. Li, and J. Yuan, "A compact fourth-order tunable bandpass filter based on varactor-loaded step-impedance resonators," *Electronics*, Vol. 12, 2539, 2023..
16. Xiang, Q., H. Sun, M. Fu, Q. Jin, and Q. Feng, "A 5th-order constant bandwidth tunable bandpass filter with two cascaded trisection structures," *IEEE Transactions on Circuits and Systems II: Express Briefs*, Vol. 70, No. 1, 126–130, Jan. 2023.